

Low hazard refractive index and density-matched fluid for quantitative imaging of concentrated suspensions of particles

W. Zhu¹ · Y. Knapp² · V. Deplano¹

Received: 15 September 2015 / Revised: 11 March 2016 / Accepted: 13 March 2016 / Published online: 27 April 2016
© Springer-Verlag Berlin Heidelberg 2016

Abstract A novel refractive index and density-matched liquid–solid suspension system taking into account chemical hazard and health concerns was developed and characterized. The solid phase is made of PMMA spheres, the refractive index of which being adapted with a mixture of 2,2'-thiodiethanol and phosphate-buffered saline (PBS), while the density is adapted with a mixture of PBS and glycerol. The proposed chemicals present low hazard characteristics in comparison with former solutions. Data collected from density and refractive index measurements of the solid phase and of the different fluid constituents are used to define a specific ternary mixture adapted to commercial grade micron-size particles. The defined mixture is validated in a micron-sized granular flow experiment. The described method can be applied to other low-density solids.

1 Introduction

Refractive index matching (RIM) techniques are often used in the qualitative or quantitative study of bounded flows (see reviews by Isa et al. 2010; Wiederseiner et al. 2011; Saksena et al. 2015) in order to avoid scattering of light at solid–liquid or liquid–liquid interfaces. In these common situations in experimental fluid mechanics, the refractive index (RI) of the fluid is adapted to the RI of the

experimental setup (walls, internal sections, porous media solid phase . . .) and to the suspending material. These techniques are implemented to reduce image distortion and to eliminate optical “hot spots” resulting from total internal reflection of illuminating light beams. While applying corrective post-processing can be considered in some limited cases, these solutions are not possible in the case of light sheet transmission for planar imaging (PIV, PTV, pLIF), for deformable liquid–liquid interfaces or for flow of suspensions. In the first case, the light path is disturbed for illumination and image acquisition, and in the two latter cases random image distortions happen due to random location of interfaces in the flow. Moreover, in such cases, RI mismatch resulting phenomena become critical when downsizing experiments to the microscale: the radii of curvature of structures and/or particles become very small, and the average number of interfaces increases. A precise RIM has therefore to be implemented. On the other hand, in the case of small-scale suspension flows, density matching (DM) becomes also a key issue. The settling velocity due to density mismatch between the different phases can lead to unwanted particle distribution/gradients. A precise DM technique has therefore to be implemented. Solving this issue reduces the number of candidates for the solid phase of the suspension because of the limited high-density fluid candidates; typically, only low-density polymers can be considered.

Historically, a great variety of recipes have been developed to match the RI of a fluid with the one of various transparent materials; see Wiederseiner et al. (2011) for a review on solid–liquid matching and Saksena et al. (2015) for a review on liquid–liquid matching. We here limit our considerations to the matching of transparent solid materials: low- or high-density polymers, glasses, fused quartz.... According to this

✉ Y. Knapp
yannick.knapp@univ-avignon.fr

¹ Aix-Marseille Université, CNRS, Ecole Centrale Marseille, IRPHE UMR7342, 13384 Marseille, France

² LAPEC EA4278, Avignon Université, 84000 Avignon, France

literature the precise RIM can be obtained by mixing different liquids (water, natural or mineral oils, organic liquids as, for example, in Lyon and Leal 1998) or by dissolving salts in water or other solvents (typ. iodide or sodium derivatives are classical candidates as in Bai and Katz 2014). In most cases, the matching is obtained by mixing adequate proportions of different components and concentration is therefore considered as the primary tuning parameter. However, these components and their mixtures have a non-negligible RI temperature coefficient (or thermo-optic constant). The mixtures are then also tunable to the sought RI by a temperature control of the experimental setup. Even if a lot of recipes have been implemented, most of the usual liquids undergo restrictions in usage and disposal due to:

- Life span issues: Iodide solutions, for example, are photosensitive and become yellow, and natural evaporation of solvents modifies the fluid properties,
- Toxicity and/or harmful health effects: Most of the salts are skin and/or eye irritants, tetralin or turpentine, Triton X100, and others are classified as toxic to aquatic life with long-lasting effects, and 1,6-dibromohexane, for example, is classified as “Fatal if swallowed”,
- Chemical interaction with the experimental setup or during storage: Potassium thiocyanate becomes red in contact with iron and has a high-RI temperature coefficient, bromocyclohexane is a solvent for PMMA, tetralin or decalin forms potentially explosive peroxides on long-time storage in contact with air/light/heat,
- Volatility, flammability: Kerosene or decahydronaphthalene, for example, has low flash point temperature and needs non-sparking tools and equipment, ventilated rooms.

Some of the raw materials even combine several of such restrictions. A principal goal of our research work was therefore to identify a novel recipe able to overcome as much as possible these limitations. From the many raw materials used for RIM, no attention has been put on the use of 2, 2'-thiodiethanol (TDE) which yet is a clear non-toxic liquid substance capable of matching the RI on a large range when mixed with simple solvents (e.g., water). The goals of the present study are (1) to present an original mixture based on TDE able to match both the RI and the density of commercial PMMA microspheres, (2) to present a simple experimental methodology and models that enable the determination of a recipe of the mixture, (3) to implement the resulting recipe in basic microscopic experiments.

2 Materials and methods

2.1 Materials

2.1.1 Solid phase

Since density matching is considered, only low-density materials such as polymers like PMMA, PS, PVA, PDMS for the solid phase should be considered. PMMA is then a good candidate since it is a widely available and low-cost material. In addition, PMMA has interesting properties: as a bulk material it can be easily bonded or machined into various geometries and exists as raw material in various shapes (rods, tubes, plates, beads). Although it is a widely used and studied material, the physico-chemical properties of commercial grade PMMA can vary in large proportions. The RI of PMMA varies in the range [1.264–3.46] median 1.4916 (Courtesy of NIMS Data Base) mainly depending on the temperature and the wavelength under consideration. Its density varies in the range [1.11–1.58] median 1.193 (Courtesy of NIMS Data Base) depending on the commercial grade of the material. Typical values found in the literature are 1.49 as RI and 1.18 as density. In the present work monodisperse PMMA particles (microparticles GmbH), with diameter $d_p = 41 \mu\text{m}$, are chosen as the solid phase of the suspension. Although these particles are of research grade the RI, n_p , and the density, ρ_p , are not precisely specified and are to be considered as being in the aforementioned ranges. Specific methods are therefore described and implemented to assess both values. This determination step can be ignored in case the data are accurately known.

2.1.2 Liquid phase

2, 2'-thiodiethanol (TDE) is a clear viscous liquid mainly used as a solvent. It can be mixed in any proportion with water so that any RI between 1.33 and 1.51 (for pure water and TDE, respectively) can be obtained: referring to the available literature a 86 % (v/v) TDE–water mixture can result in a 1.49 refractive index (Staudt et al. 2007). However, phosphate-buffered saline (PBS) solution has been proved to be a better solvent, increasing the stability and life span of the mixture. Adding different amounts of water or PBS will result in a modification of the density of the final mixture; the density range is then between 1 and 1.18 (for pure water/PBS and TDE, respectively). Here, a simple procedure to compensate this density reduction consists in adding a third miscible high-density material. A good candidate for such adaptation is pure glycerol which has a typical density of 1.26 and a RI of 1.47. The reduction in density can obviously be compensated by addition of glycerol with limited impact on the RI. Moreover, Material Safety Data Sheets (MSDS) of these components show that

glycerol and PBS are “Not regarded as a health or environmental hazard under current legislation.” Concerning TDE, and to the best of our knowledge, the MSDS present only a hazard warning about high irritation in case of eye contact; wearing eye shields is highly recommended. Another interesting feature of the proposed mixture is its RI temperature coefficient. The coefficients reported in the literature for the different constituents of the mixture are around $-2 \cdot 10^{-4}/^{\circ}\text{C}$ for glycerol, $-3 \cdot 10^{-4}/^{\circ}\text{C}$ for TDE and $-1 \cdot 10^{-4}/^{\circ}\text{C}$ for water/PBS. A mixture of these components should therefore result in a RI and density-matched suspension with a refractive index temperature coefficient differing from the reported value of about $-1 \cdot 10^{-4}/^{\circ}\text{C}$ for PMMA. This will allow for a proper adjustment of the RI of the liquid to a desired value by changing its temperature.

2.2 Experimental methods

2.2.1 Mixture definition methodology

Once n_p and ρ_p are determined, it is possible to proceed to the definition of the proper recipe based on the aforementioned components. While usually the preparation of a ternary mixture is based on the assembly of two solutions having a common component, the preparation protocol is here simplified as following: at first a mixture of glycerol and PBS is prepared, noted as solution A. Then an amount of solution A is mixed with pure TDE (noted solution B) to obtain the final mixture solution C which is designed to match the density and RI of the particle at a set temperature. This procedure limits the study to a small range of concentrations and temperatures. Thereby, the proportion of glycerol in solution A and of TDE in solution C will be calculated from Eqs. (1) and (2) for a given temperature.

$$\begin{cases} \rho_A = f_1(T, \chi), & n_A = f_2(T, \chi) \\ \rho_B = f_3(T), & n_B = f_4(T) \end{cases} \quad (1)$$

$$\begin{cases} \phi \cdot n_B + (1 - \phi) \cdot n_A = n_C \\ \phi \cdot \rho_B + (1 - \phi) \cdot \rho_A = \rho_C \end{cases} \quad (2)$$

where ϕ is the volume fraction of TDE, χ is the mass fraction of glycerol in solution A (mixture of glycerol and PBS), ρ_A, n_A are density and RI of solution A, ρ_B, n_B are density and RI of TDE, ρ_C, n_C are density and RI of solution C. The equation set (1) and the underlying functions f_1, f_2, f_3, f_4 are obtained by linear regressions of measured data. Equation set (2) is based on the hypothesis that both the RI and the density of the mixture follow an Arago–Biot-type equation. The evolution of RI and density of solution A as a function of glycerol proportion and temperature, and the evolution of RI and density of TDE as a function of temperature are necessary input data for the resolution of the system.

2.2.2 Properties of the solid phase

2.2.2.1 Refractive index A method based on absorbance/transmission was implemented to measure the RI of the small PMMA particles (Wiederseiner et al. 2011). For this, a modified commercial spectrophotometer (Uviline 9400, Secomam) was used. The modifications consisted in the implementation of a specific thermal control of the sample cells and the addition of a pinhole on the light path at the output of the wavelength-controlled light source. Temperature-controlled absorbance measurements at a typical 589 nm were taken on PBS/TDE solutions with various concentrations containing about 8 % particles (w/w). For each solution a measurement of the RI (temperature-controlled Abbe refractometer) was taken at the same wavelength so that the minimum absorbance concentration could directly be converted in a RI of the particles. This minimum was inferred from the derivation of a parabolic curve matching the measured data points. Note that this method results in the determination of the RI of the particles at a given temperature. This temperature should be used as input data for the resolution of Eqs. (1) and (2). If necessary this method can be repeated for various PBS/TDE mixtures so that the RI can be determined at different temperatures. This time-consuming work can be avoided by considering the temperature dependence of refractive index of PMMA which is $-1.09 \cdot 10^{-4}/^{\circ}\text{C}$ in the range of implemented temperature and wavelength following Kasarova et al. (2010).

The accuracy of the method relies on the thinness of the dilution steps. However, in the present work the dilution steps and their precision were very small and the principal source of error comes from the refractive index measurement apparatus and procedure. The resulting accuracy thereof was ± 0.0003 .

2.2.2.2 Density Because the settling velocity of particles can be very low when the matching gets close, the density of the particles is determined indirectly by a centrifugation procedure. Mixtures of water and glycerol with different concentrations obtained by consecutive dilutions of an initial solution serve as a suspending material for the particles. The density of the water–glycerol solutions is determined from the dilution process by weighing, initial densities being determined with a pycnometer. The water–glycerol particle mixtures are sampled with small 70 μm internal diameter and 50 mm long glass capillaries. The capillaries are centrifuged 12 min at 16,000 $\times g$ before analysis under a microscope. The difference of density between liquid and solid phase results in a clear separation toward the inner or outer direction of the centrifuge. The accuracy of the method relies on the thinness of the dilution steps; in the present case this accuracy was $\pm 0.0012 \text{ g/cm}^3$ as the half of the density difference between two consecutive dilutions, each inducing an opposite separation of particles after centrifugation.

2.2.3 Properties of the liquid phase

2.2.3.1 Refractive index A traditional Abbe refractometer is used to measure the RI of different liquid samples. The refractometer works based on the optical refraction critical angle detection technique and has a measuring range of 1.3–1.7, a resolution of $0.0005n$ and an accuracy of $\pm 0.0003n$ ($\pm 0.15\%$). In order to control the temperature of the samples, the refractometer was connected to a thermal regulation system (Fisher Scientific Isotemp circulator with water running through it as the working fluid) with a temperature stability of $\pm 0.1\text{ }^\circ\text{C}$.

2.2.3.2 Density For the measurement of the density of liquids, a density meter (Anton Paar) was used. The device can simultaneously measure the temperature and the density of the test medium. The accuracy of the measurement is 0.001 g/cm^3 at temperature accuracy $0.2\text{ }^\circ\text{C}$. In order to limit experiments, 4 mixtures of glycerol and water with densities potentially close to an average 1.18 g/cm^3 are presented. These mixtures have, respectively, 68, 70, 72 and 75 % glycerol mass fractions. The density and refractive index of these solutions and of pure TDE were measured at different temperatures from 18 to $30\text{ }^\circ\text{C}$.

3 Results and discussion

3.1 Results of PMMA particles measurement

3.1.1 Refractive index

The RI of PBS (Fisher Scientific) and TDE (Sigma-Aldrich) mixtures at different temperatures was already determined (data not shown), and a direct transformation gives the relation between relative absorbance and RI measurements (Fig. 1).

According to these data, a parabolic curve fit is applied to each dataset with a coefficient of determination $R^2 = 0.9908$, valid for $T = 16\text{--}32\text{ }^\circ\text{C}$. A derivation of the curves gives access to the minimum of the curve for which the RI of fluid and particles is matched. From this method the average RI of the particle is $n_p = 1.4892 \pm 0.0003$ at wavelength 589 nm at $22.25\text{ }^\circ\text{C}$. The accuracy of the method is imposed by the accuracy of the RI measurements. The obtained RI value is consistent with the measurement of Wiederseiner et al. (2011) 1.48847 (0.04 % difference) and with the value 1.4934 (0.28 % difference) inferred from the work by Kasarova et al. (2010). Such slight discrepancies are reasonable considering possible differences in composition and/or manufacturing process.

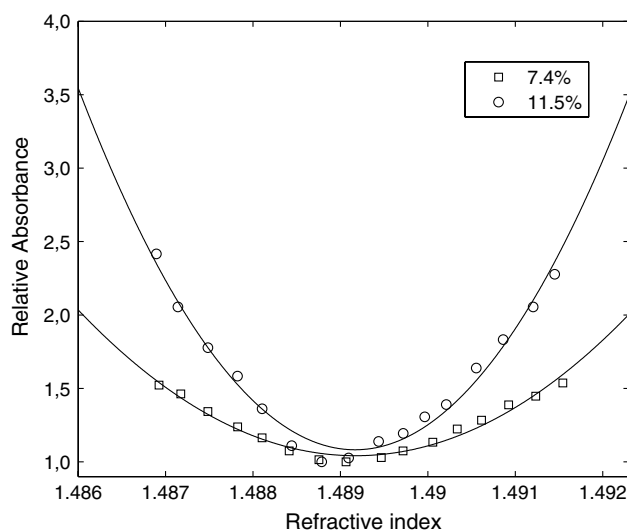


Fig. 1 Relative absorbance as a function of RI for 2 PMMA suspensions in mixtures of PBS and TDE. Measurement is done by variation of temperature

3.1.1.1 Density The application of the procedure described in Sect. 2.2.2 and the observation of the capillaries tips under a microscope resulted in clear density separations. For the present case, particles have moved toward the centrifuge outer direction in the solution with a density of 1.1866 g/cm^3 (glycerol mass fraction of 73.96 %), and particles have moved toward the centrifuge inner direction in the solution with a density of 1.1890 g/cm^3 (glycerol mass fraction of 73.1 %). The density of the particle is therefore between these two density values. The resulting density value for the particles is inferred from the average of these two values, and the accuracy can be inferred from the extreme values of the densities in each tube. Therefore, $\rho_p = 1.1878 \pm 0.0012\text{ g/cm}^3$ at $22\text{ }^\circ\text{C}$. Note that when compared to the natural sedimentation method (1 week), the present method is far less time-consuming (12 min) with a similar accuracy.

3.2 Results of fluid component properties

3.2.1 Refractive index

Figure 2 shows n_A as a function of temperature for different glycerol mass fractions.

A multiple linear regression on these data gives the following dependency:

$$n_A = 0.1425\chi - 0.00023T + 1.3321 \quad (3)$$

with $R^2 = 1$, valid for $T = 16\text{--}30\text{ }^\circ\text{C}$ and at glycerol mass fractions $\chi = 68, 70, 72, 75\%$.

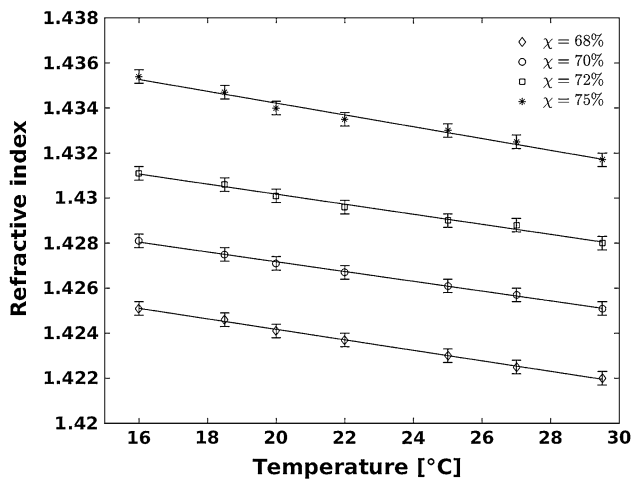


Fig. 2 RI of glycerol–PBS mixtures $n_A \pm SD$ as a function of temperature for glycerol mass fractions $\chi = 68, 70, 72, 75\%$

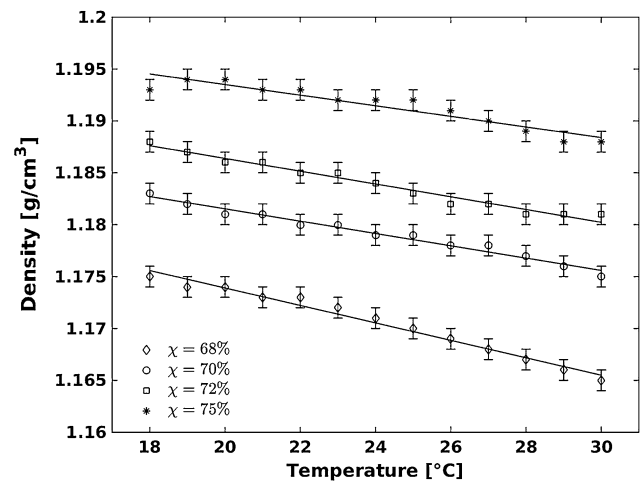


Fig. 4 Density of glycerol–PBS mixtures $\rho_A \pm SD$ as a function of temperature for glycerol mass fractions $\chi = 68, 70, 72, 75\%$

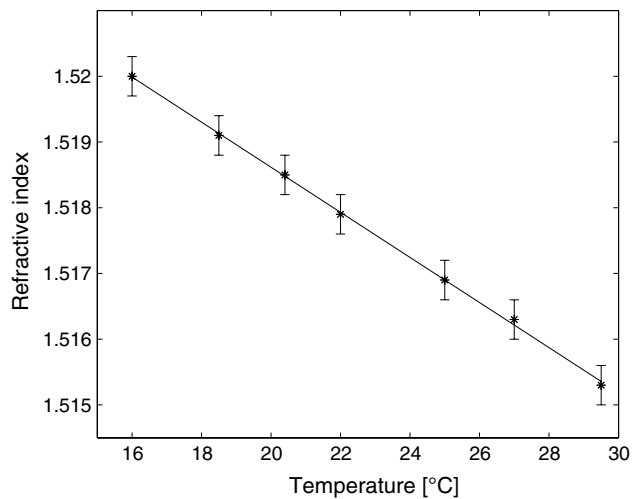


Fig. 3 RI $n_B \pm SD$ of pure TDE as a function of temperature

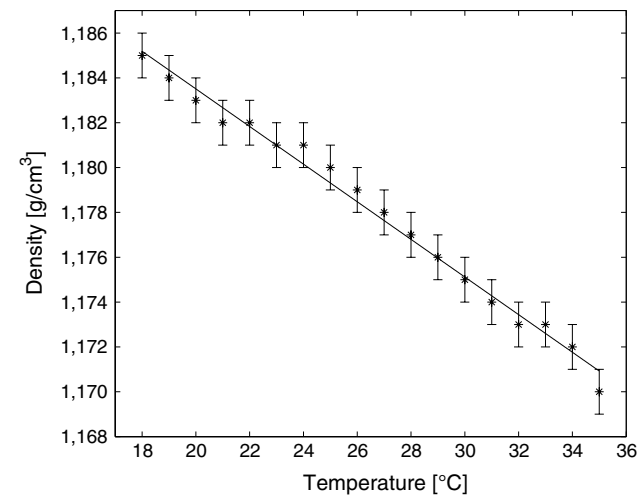


Fig. 5 Density $\rho_B \pm SD$ of pure TDE as a function of temperature

The RI of TDE was measured from 15 to 30 °C. Results are shown in Fig. 3, and a simple linear regression analysis of the data results in Eq. (4), with $R^2 = 0.9977$:

$$n_B = -0.00034T + 1.52548 \tag{4}$$

3.2.1.1 Density Figure 4 shows the density of solution A as a function of temperature for different glycerol mass fractions.

A multiple linear regression of these data gives Eq. (5) with $R^2 = 0.9765$ which is valid for $T = 18\text{--}30\text{ }^\circ\text{C}$ and glycerol mass fractions $\chi = 68, 70, 72, 75\%$.

$$\rho_A = 0.2917\chi - 0.00065T + 0.989 \tag{5}$$

Measurements of the density of pure TDE were performed, and the resulting data are presented in Fig. 5 as a function of temperature.

A simple linear regression analysis of the measured data gives Eq. (6) with $R^2 = 0.9887$ which is valid for $T = 18\text{--}30\text{ }^\circ\text{C}$.

$$\rho_B = -0.00084T + 1.20029 \tag{6}$$

3.2.2 Determination of the recipe

From the above measurements, the equation set (1) can be rewritten as follows.

$$\begin{cases} \rho_A = 0.2917\chi - 0.00065T + 0.989 \\ n_A = 0.1425\chi - 0.00023T + 1.3321 \\ \rho_B = -0.00084T + 1.20029 \\ n_B = -0.00034T + 1.52548 \end{cases} \tag{7}$$

As the RI and density of the particles were already measured, the recipe can be estimated according to Eq. (8), rewritten from Eq. (2) with the preceding dependencies.

$$\begin{cases} \phi \cdot n_B + (1 - \phi) \cdot n_A = n_C = n_P = 1.4892 \\ \phi \cdot \rho_B + (1 - \phi) \cdot \rho_A = \rho_C = \rho_P = 1.1878 \end{cases} \quad (8)$$

A recipe can be inferred from both sets of equations by fixing at least one parameter. As an example one can consider straightforwardly that the choice of temperature is dictated by the temperature at which the RI and density were determined, which is 22 °C. Considering this temperature in Eq. (7) and substituting in Eq. (8) results in $\phi = 64\%$, $\chi = 77\%$. A closer insight into Eq. (8) shows that although the matching relies on both fractions of glycerol in PBS and of TDE in the final mixture, a fine-tuning can be obtained by adjusting the temperature. In particular, a sensitivity analysis of the equation for the refractive index shows that a 2 % error in both fractions can be compensated by a variation of about 6 °C which is quite reasonable and technically realizable in most cases. Note that such a variation affects poorly the RI of the PMMA solid phase with only 0.0087 % variations.

3.3 Trial experiments of the recipe

3.3.1 Static experiments

A mixture, following an identified recipe, was prepared, and particles were added (40 % v/v) before static observation under a microscope (Olympus IX71, Japan). The observations were made through a 1 mm fluid thickness and tried to image a grid from a standard stage micrometer (Edmunds Optics). A $\times 20$ – NA = 0.5 objective lens allowed to have a depth of field $\text{DOF} = 2.2 \mu\text{m}$. The system was placed in a temperature-controlled climatic chamber. Images of the grid were taken for stabilized temperatures in the range $T = 14$ – 32 °C. A clear and sharp image of the grid can be obtained in the case of particle-free mixture (Fig. 6a). The great number of potential optical interfaces (approx. 50 in the present case) results in an impossibility to image the grid in case of unmatched RI (Fig. 6b). A better image quality is obtained when the RI is matched (Fig. 6c, d). In order to determine the temperature for which the best focus of the grid is observed, a diagonal Laplacian focus measure was computed on the images (Pertuz et al. 2013). The relative maximum of this measure allowed to identify the temperature for which the best focus is obtained (Fig. 6d). The identified temperature was in good agreement with the temperature used for the initial condition of equation set (7).

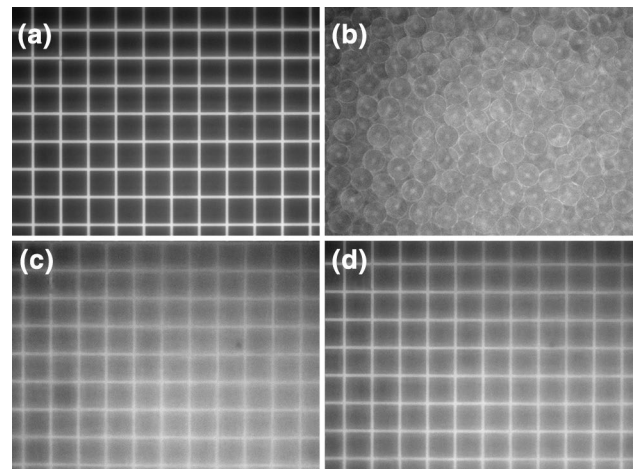


Fig. 6 Image of a grid from a standard stage micrometer with various 1 mm thick interfaces: **a** fluid mixture without particles, **b** 41 μm particles in water, **c** 41 μm particles in fluid mixture at 24 °C, **d** 41 μm particles in fluid mixture at 20 °C

3.3.2 Dynamic experiments

The in-focus image obtained with particles (Fig. 6d) is not as clear as the one without particles (Fig. 6a). Therefore, it is important to quantitatively assess the quality of the suspension in a dynamic experiments. To do so, the prepared mixture was tested in a simple shearing flow generated in the gap of a rotating cone-plate geometry placed above the microscope (same optical system already described). The rotating cone has a 80 mm diameter and 2° angle. The optical window through which optical measurements were taken is placed on a radius of 30 mm from the rotation center. The resulting gap between the cone and the fixed lower plate at this radius is equal to 1047 μm . The data presented hereafter correspond to a shear rate value of 50 s^{-1} , a Reynolds number of 1.22 according to a mixture viscosity of 51 mPa s at 22 °C. Two particle concentrations, 0 and 45 % v/v, were considered, and the most unfavorable plane located at 900 μm from the fixed bottom plate was chosen for the demonstration of the optical quality of the developed suspension. Microparticle image velocimetry, μPIV (Wereley and Meinhardt 2010), measurements were realized in different planes along the gap height. The suspension was seeded with 1 μm fluorescent particles (FluoSpheres F8819, Invitrogen, France) and illuminated in volume by a double-pulsed 532 nm laser light (NdYag Gemini PIV, New Wave Research, USA) through the fixed lower plane. The concentration of seeding particles was set to 0.031 % v/v (Wereley and Meinhardt 2010). The 575 nm emitted light from the seeding particles is filtered by a proper separating cube placed in the microscope. Image pairs of the flow were taken with a 12-bit cooled 1.4 Mpixel digital CCD

camera system (Sensicam qe, PCO, Germany). The depth of correlation was equal to $11.6\ \mu\text{m}$, and the field of view was $894 \times 665\ \mu\text{m}^2$. As an example, Fig. 7a, b compares representative images of $192 \times 192\ \text{pix}^2$ windows extracted from the complete image and their corresponding cross-correlation functions obtained from highlighted $64 \times 64\ \text{pix}^2$ interrogation windows. When considering a simple FFT-based cross-correlation computation (1302 vectors resulting from 50 % overlapping, $64 \times 64\ \text{pix}^2$, interrogation windows with a Gaussian weighing) on a single image pair, a 48 % signal-to-noise ratio (SNR) rejection of the cross-correlation is observed for the 45 % suspension versus 10 % in the case of 0 % concentration. This rejection comes from a poor peak to noise peak ratio (PNPR) in the peak detection algorithm. This ratio computes the peak pixel intensity divided by the highest noise peak pixel intensity. Its threshold value was strictly set to 1.5. When the cross-correlation is not rejected (distinct peaks observed in Fig. 7a, b), the average PNPR over the 52 % valid peaks is 1.98 (respectively, 2.38 for the 95 % valid peaks for 0 %). PNPR is an indicator of the image quality since it is a metric of the combination of (1) the effects of the number of seeding particles present in the interrogation window and of their mean image diameter and (2) the effects that contribute to loss of correlation (in-plane and out-of-plane loss of correlation) (Raffel et al. 2007). Since the fluid is highly viscous and the flow is laminar, the out-of-plane loss of correlation is strongly limited. Furthermore, the pulse separation time was carefully adjusted to fulfill the gold standard rule of an average displacement of about one quarter of the interrogation window size (typ. about 16 pixels here for a pulse separation of $200\ \mu\text{s}$). This setting results in a limited in-plane loss of correlation. 0 % experiment shows a very good performance with similar

seeding conditions than the 45 % suspension, and the high rejection outcome is therefore mainly related to a loss of image density and/or to small particle image diameter in the interrogation windows when considering high-concentrated suspension. Consequently, rejection can be linked to the small radius of curvature of PMMA particles, the large number of interfaces present in the concentrated suspension and to potential residual RI mismatch. Different solutions can be considered to overcome these issues; for example, a less restrictive rejection ratio, image pre-processing and ensemble-averaged cross-correlation algorithm. This latter solution was implemented. The magnitude of the displacement field at a given height in the flow was determined from computing ensemble-averaged cross-correlations from 30 image pairs (Wereley and Meinhardt 2010). This procedure improves drastically the performance of the cross-correlation peak detection measurements. Only 5 % of the cross-correlation do not pass the SNR filter (same PNPR threshold as above) for the 45 % suspension (respectively, 0.3 % for the 0 % suspension). Moreover, the average PNPR is then 2.67 (respectively, 4.33) improving therefore the displacement determination from the cross-correlation computation.

The obtained displacement magnitude fields for the 0 and 45 % suspension are shown in Fig. 7c, d. Fields differ mainly by their standard deviation (STD): 0.097 pixels in the case of the 45 % suspension and 0.013 pixels in the case of the 0 % suspension. STD values are however small when compared to the mean value of the displacement field (13.94 pixels and 14.08 pixels for 0 and 45 %, respectively). The standard deviation represents 0.7 % of the average displacement in the case of the 45 % suspension (respectively, 0.09 for 0 %). In both cases, the implemented procedures give excellent results.

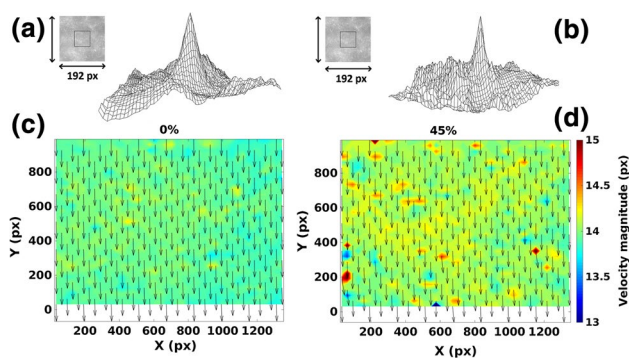


Fig. 7 μPIV experiments. *Top* images of $192 \times 192\ \text{pix}^2$ windows taken in the image and the corresponding cross-correlation functions obtained from highlighted $64 \times 64\ \text{pix}^2$ interrogation windows for two PMMA particle concentrations. **a** 0 % v/v and **b** 45 % v/v. *Bottom* magnitude of displacement fields [pixels] obtained from ensemble-averaged cross-correlation from 30 image pairs for two PMMA particle concentrations. **c** 0 % v/v and **d** 45 % v/v

4 Conclusion

TDE a novel, low hazard pure fluid has been used as a principal constituent to define a mixture able to match the density and refractive index of transparent low-density PMMA particles. A simple method, based on the resolution of a set of linear equations, has been shown to be able to identify a recipe for the definition of volume fractions of a ternary mixture of TDE, glycerol and PBS. The proposed method shows that a low accuracy in the preparation of the mixture can be corrected by adjusting the temperature of the mixture. The performance in matching the refractive index of the mixture has been demonstrated in a static and in a dynamic flow experiments.

A large range of RI and densities can be achieved by varying the concentration of the three chosen components. Moreover, other secondary components can be considered

to fulfill specific needs; TDE is soluble in a lot of solvents. This range will however be limited to transparent solid low-density materials, mainly because of the difficulty to find high-density transparent liquids with low toxicity. The main drawback of the proposed mixture lies probably in its high Newtonian viscosity. This point will probably limit the implementation of this mixture to low Reynolds number flows. The proposed mixture can finally be considered as another versatile solution for the precise determination of RI of transparent solids, in replacement of other common recipes (Bai and Katz 2014).

Acknowledgments The authors thank the Labex MEC ANR-11-LABX-0092 for financial support.

References

- Bai K, Katz J (2014) On the refractive index of sodium iodide solutions for index matching in PIV. *Exp Fluids* 55(4):1704
- Isa L, Besseling R, Schofield AB, Poon WCK (2010) Quantitative imaging of concentrated suspensions under flow. In: *Advances in polymer science: high solid dispersions*, vol 236, pp 163–202
- Kasarova SN, Sultanova NG, Nikolov ID (2010) Temperature dependence of refractive characteristics of optical plastics. *J Phys Conf Ser* 253:012028
- Lyon M, Leal L (1998) An experimental study of the motion of concentrated suspensions in two-dimensional channel flow. Part 1. Monodisperse systems. *J Fluid Mech* 363:25–56
- Pertuz S, Puig D, Garcia MA (2013) Analysis of focus measure operators for shape-from-focus. *Pattern Recogn* 46:1415–1432
- Raffel M, Willert CE, Wereley ST, Kompenhans J (2007) *Particle image velocimetry: a practical guide*, 2nd edn. Springer, Heidelberg
- Saksena R, Christensen KT, Pearlstein AJ (2015) Surrogate immiscible liquid pairs with refractive indexes matchable over a wide range of density and viscosity ratios. *Phys Fluids* 27:087103-1-21
- Staudt T, Lang MC, Medda R, Engelhardt J, Hell SW (2007) 2, 2'-Thiodiethanol: a new water soluble mounting medium for high resolution optical microscopy. *Microsc Res Tech* 70(1):1–9
- Wereley ST, Meinhardt CD (2010) Recent advances in micro-particle image velocimetry. *Annu Rev Fluid Mech* 42:557–576
- Wiederseiner S, Andreini N, Epely-Chauvin G, Ancey C (2011) Refractive-index and density matching in concentrated particle suspensions: a review. *Exp Fluids* 50(5):1183–1206